AN EXPERIMENTAL STUDY FOR AERODYNAMIC AND ACOUSTIC EFFECTS OF ON-BLADE ACTIVE TAB

Kobiki Noboru
Shigeru Saito
JAXA
(Japan Aerospace Exploration Agency)
Tokyo, Japan

Takeshi Akasaka
Yasutada Tanabe
Kawada Industries, Inc.
Tochigi Pref., Japan

Hiroaki Fuse
Nihon University
Tokyo, Japan

Abstract

This paper presents the outline of the active tab research/development program and the experimental results of the active tab effect on rotor noise reduction and blade pressure characteristics. The active tab is installed in a blade of a 1-bladed rotor model and the blade pressure and the noise reduction effect is studied by a wind tunnel test measuring blade surface pressure and sound pressure in order to evaluate the correlation between aerodynamic and acoustic effects for a control law development for the active tab. The active tab effect is studied with respect to the active tab phase angle. About 2dB noise reduction is observed from the base line condition where the active tab is not operated and about 3dB capability to control the rotor noise, which is the difference between the maximum and the minimum rotor noise, is also demonstrated. A close correlation between blade pressure characteristics and rotor noise is observed, which implies that the blade surface pressure can be a promising index to detect BVI and to evaluate the active tab effect on BVI reduction.

Notation

Symbols

c	Blade chord=0.12m
C_p	Pressure coefficient
ΔC_{pmax}	Pressure fluctuation index
R	Rotor radius=1m
SPL	Sound pressure level (dB)
V_W	Wind tunnel speed (m/sec)
δ_{AT}	Active Tab deflection (deg.)
ψ	Rotor azimuth angle (deg.)

Abbreviations/Subscripts

AT	Active Tab
BVI	Blade/Vortex Interaction

Introduction

Having VTOL and hovering capabilities, helicopters are used in a various scenes where we can realistically feel the utility of helicopters, such as ambulance, rescue, news reporting, transportation, security and so on. But due to the noise problems, helicopters can be operated only a constrained conditions, which can be noted that helicopters have not been fully made use of their versatile ability.

The technological solutions have long been desired which can obtain public acceptance by highly reducing the noises emitted around heliports and beneath flight paths and can clear ICAO noise regulation getting more stringent with sufficient margin.

Among the noised generated by helicopters, the BVI noise causes significant noise damage and can not be well reduced by passive techniques such as airfoil/tip shape improvement. In order to resolve this BVI noise problem, many research organizations and helicopter manufactures have been working to research/develop BVI noise reduction techniques for these decades as one of the high priority technical tasks.

The most promising technique so far seems to be active flap which is one of active techniques. Active flap drives a small flap installed at the trailing edge of a blade tip portion as shown in Fig.1.

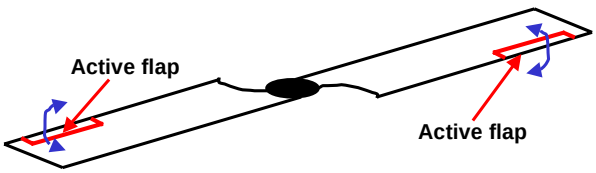

Fig.1 Active Flap

This technique is power effective,

because only the aeroacoustically useful blade tip part is driven. The flap is actuated by an on-board smart actuator. This technique is materialized by a recent breakthrough in the smart actuator technology area. Although the flap drive system still has the challenges in a mechanical component to make enough large flap amplitude with high frequency in high centrifugal force circumstance, ATIC (Advanced Technology Institute of Commuter-helicopter) for the first time demonstrated the capability of the active flap by carrying out a whirl tower test with a full scale active flap installed on a rotor (Ref.1). Boeing successfully performed a whirl tower test with full scale active flap recently (Ref.2) and Eurocopter is reported to carry out soon a flight test with active flap (Ref.3).

Control laws applicable to active technique corresponding to time varying flight conditions and able to generate proper set of operating quantities such as frequency, amplitude and phase are also essential and have been developed briskly (Ref.4).

On these backgrounds, JAXA (Japan Aerospace Exploration Agency) and Kawada Industries Inc. have been working to research and develop a new active technique for helicopter noise reduction which is available to ICAO defined flight patterns, namely approach, fly over and take-off. This new technique is referred as “Active Tab”.

The outline of this research program is depicted in Fig.2. We started in 2002 to study the fundamental tab aerodynamic property by a 2D static wind tunnel test, then proceeded to 2D dynamic wind tunnel test in 2003 to examine the tab dynamic effect. This step of the study showed that a realistic size and anhedral of the active tab has sufficient aerodynamic capability equivalent to the potential for rotor noise reduction (Ref.5). CFD analysis simultaneously started to propose aerodynamically effective tab geometry (Ref.6).

In 2004, the rotor wind tunnel test was carried out in a rotor configuration with on-blade active tab to evaluate the active tab effect on rotor noise reduction and to provide the validation data for CDF code development. It is demonstrated by this wind tunnel test in a rotor configuration that the active tab has the efficient capability to control the rotor noise about 3dB and that the active tab is one of the promising techniques for rotor noise reduction (Ref.7).

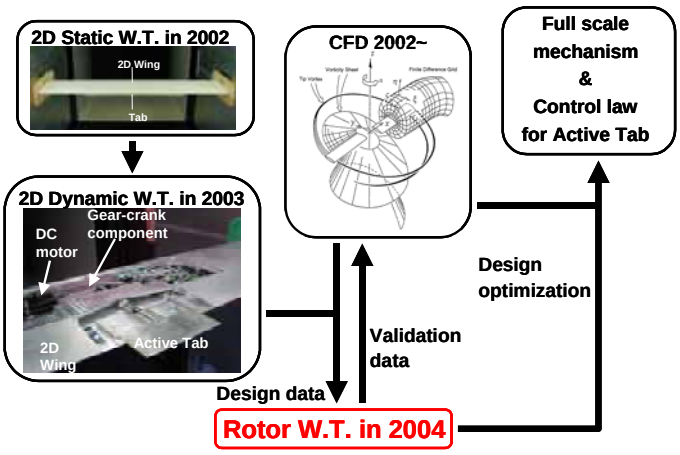

Fig.2 Active Tab research program

This paper presents the understandings for blade aerodynamic characteristics and noise reduction effect obtained by the active tab wind tunnel test in a rotor configuration.

Objectives

The objectives of this study are as follows;

1. Study for blade aerodynamic influences induced by Active Tab to pursue effectiveness for noise reduction purpose.

2. Evaluation for the correlation between aerodynamic and acoustic effects by Active Tab for control law development.

Description of Active Tab

The schematic view of the active tab is shown in Fig.3. The active tab is installed in the aft portion of the airfoil and driven back and forth dynamically to reduce BVI noise and the vibration by the blade lift control due to the variable blade area effect.

The active tab also can be operated statically, such as the active tab is deployed with some displacement and fixed. This way of operation can increase the blade lift during the whole revolution of the blade so that the rotor speed can be reduced by making use of this lift increment, which has the effect on the climb and fly-over noise reduction.

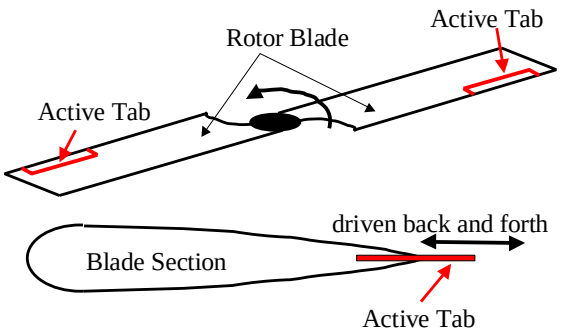

Fig.3 Active tab concept

Wind Tunnel Testing

Model description

This wind tunnel test was performed to study the noise reduction effect of the active tab by a rotor configuration in the 2.5x2.5m low speed wind tunnel of Kawada Industries, Inc. using a one-bladed rotor system as shown in Fig.4. The main features of this rotor system are shown in Table 1.

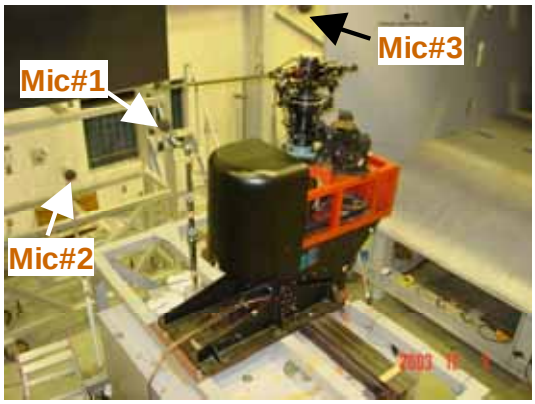

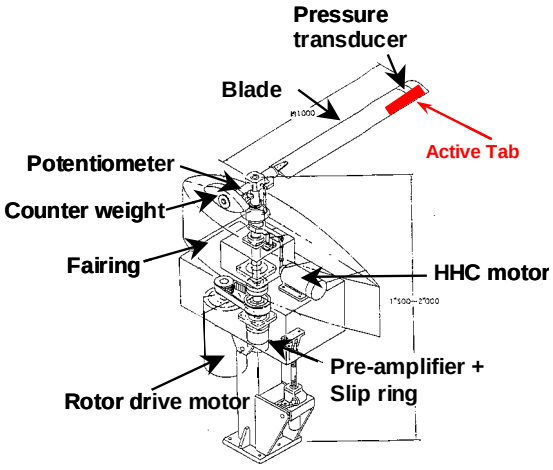

Fig.4 One-bladed rotor system

Table 1 Features of rotor system and active tab

Hub type	rigid in flap and lead-lag
Rotor radius	1m
Blade chord	0.12m
Airfoil	NACA0012
Blade plan form	Rectangular
Rotor rpm	1200rpm (max)
Collective pitch	-5 to +15deg.
Cyclic pitch	0deg. (fixed)
Active Tab	Amp. : 12mm(max)
	Freq. : 20Hz
	Phase : variable
	Span : 80 ~ 98%R

The active tab installed on the blade and its schematic drawing are shown in Fig.5. The main features of the active tab are also shown in Table 1. The tab is fan-shaped so that the extended area generated by the tab operation is made larger in the outer portion of the blade. A 10deg. anhedral angle is put to the tab so that the tab effect to the blade lift increment is augmented based on the previous work as shown in Ref.5.

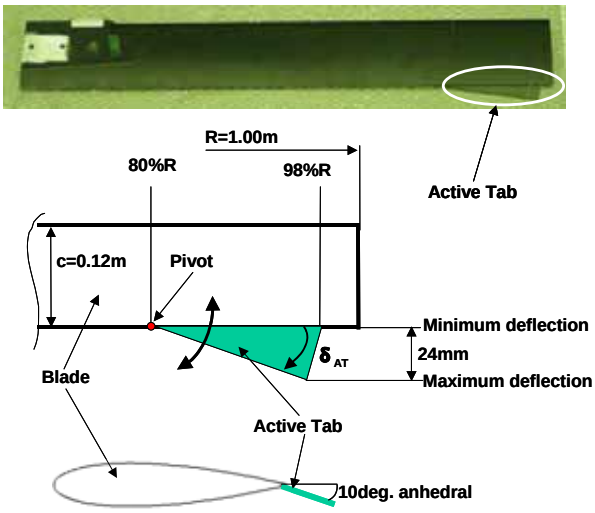

Fig.5 Active Tab installation

This active tab is pivoted at its apex to 80%R location of the blade. The end of the rack which makes the active tab move back and forth is fixed to the active tab slightly outboard side of the active tab apex so that the travel of the rack can be made as small as possible to achieve the full amplitude of the active tab motion. The other details of the rotor system and the blade with active tab are described in Ref.7.

The active tab deflection is defined as

follows;

$$\delta_{AT} = \theta_{AT} \cos(2\Omega t - \phi_{AT})$$

where

δ_{AT} : active tab deflection (deg.)

θ_{AT} : active tab amplitude (pre-set, deg.)

ϕ_{AT} : active tab phase (deg. or rad)

Ω : rotor speed (rad/sec)

Test condition

The test condition is as follows;

Wind tunnel

Wind speed : 18m/sec

Test section : open

Rotor system

Rotor speed : 600rpm (10Hz)

Collective pitch angle : 4.3deg

Cyclic pitch angle : 0deg

Rotor shaft angle : 2deg. nose up

Active tab

Frequency : 20Hz (2/rev)

Amplitude : 3.8deg.

Phase : 0 ~ 360deg.

Measurement

The schematic view of the whole measurement system is shown in Fig.6.

The blade surface pressure distribution is measured by pressure transducers mainly located on the 85%R position of the upper and lower sides of the blade. Two microphones are set in the wind tunnel as shown in Figs.4 and 7 to evaluate the active tab effect for rotor noise reduction.

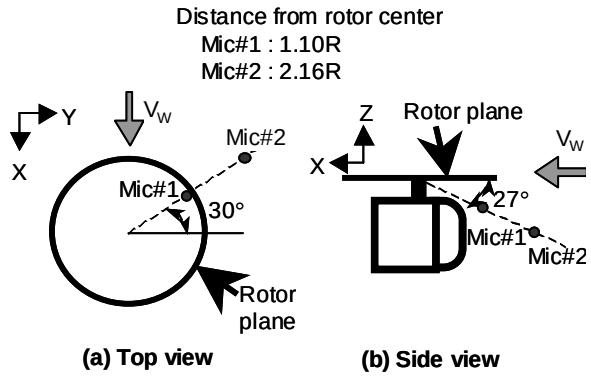

Fig.7 Microphone position

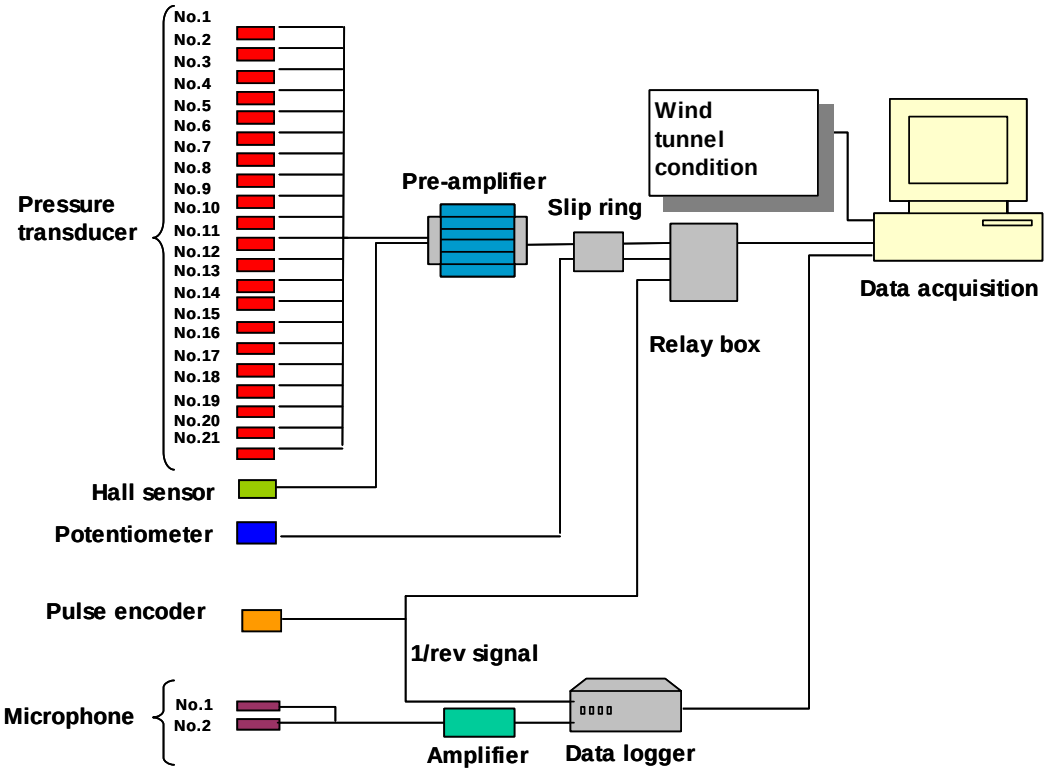

Fig.6 Measurement system

The active tab deflection is detected by a Hall sensor installed just inboard portion of the active tab and a potentiometer installed at the center of the rotor hub measures blade pitch angle. A pulse encoder generating 1/rev signals is installed beneath the rotor plane at about ψ =0deg.

Data acquisition/procession

The above mentioned measured items are acquired simultaneously and processed with 1/rev output signals of the pulse encoder in order to be related with the rotor azimuth angle.

The sample rate for microphones is set at 10kHz and that for the others such as the blade surface pressures and Hall sensor is set at 4kHz by the limitation of data storage.

All the data acquired in the time domain are ensemble averaged of 40 revolutions equal to 4sec. in order to eliminate the random noise from the measured data and to make the periodical aeroacoustic and aerodynamic characteristics caused by rotor revolution clear.

The other details of the data acquisition/procession are described in Ref.7.

Results and Discussion

Rotor noise reduction

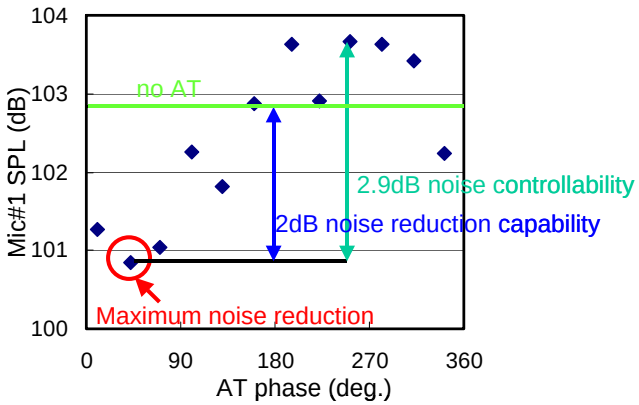

Fig.8 AT effect for rotor noise reduction (Mic#1)
V_W=18m/sec, rotor speed=600rpm, collective=4.3deg., cyclic=0deg., rotor shaft angle=2.0deg., AT frequency=2/rev, AT amplitude=3.8deg.

Fig.8 shows the active tab effect for rotor noise reduction measured by Mic#1. The sinusoidal variation of the sound pressure level with respect to AT phase is fairly seen in this figure. The background noise caused by the wind tunnel is subtracted from all the data points. Furthermore for AT on cases, the mechanical noise generated during AT operation is subtracted as well to purify the AT effect on rotor noise reduction.

AT phase=42deg. has the maximum noise reduction effect, otherwise AT phase=252deg. has the most adverse effect. 2dB noise reduction capability from no AT condition and 2.9dB noise controllability, which is the difference between the maximum and the minimum rotor noise, are observed from this figure.

Fig.9 shows the sound pressure time history measured by Mic#1 of no AT and AT with phases for maximum and minimum BVI. The upper graph of Fig.9 shows the time history over one revolution of the blade and the lower graph of Fig.9 does over interested azimuth range around BVI region.

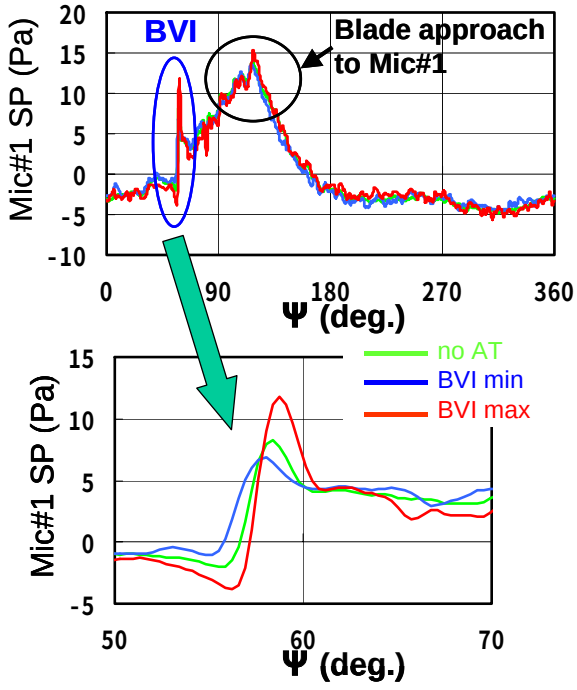

Fig.9 AT effect for sound pressure time history (Mic#1)
V_W=18m/sec, rotor speed=600rpm, collective=4.3deg., cyclic=0deg., rotor shaft angle=2.0deg., AT frequency=2/rev, AT amplitude=3.8deg.

The BVI is captured at around ψ=58deg. as a steep peak of the sound pressure in the upper

graph of Fig.9. The gentle peak of the sound pressure at around ψ=120deg. is inferred to be formed by increasing thickness and loading noise emitted from the blade as the blade approaches to the microphone which is located at ψ=120deg. as shown in Fig.7. The lower graph of Fig.9 clearly indicates the effect of AT on sound pressure as the difference of the peak-to-peak magnitudes of sound pressure at around BVI region among no AT and AT with phases for maximum and minimum BVI.

Fig.10 shows the sound pressure spectrum measured by Mic#1 of no AT and AT with phases for maximum and minimum BVI, which is the same case as Fig.9. The upper graph of Fig.10 has a wider range of frequency to overview the sound characteristics influenced by AT and the lower graph of Fig.10 does over interested frequency range around 1,000Hz where the human sense of hearing is sensitive.

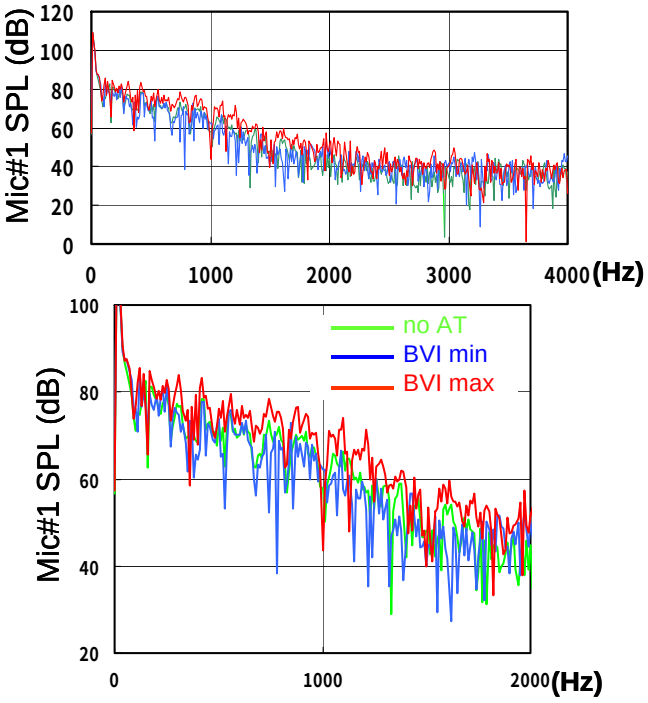

Fig.10 AT effect for sound pressure spectrum (Mic#1)

V_W=18m/sec, rotor speed=600rpm, collective=4.3deg., cyclic=0deg., rotor shaft angle=2.0deg., AT frequency=2/rev, AT amplitude=3.8deg.

Fig.10 shows that the sound pressure spectrum also has a tendency for AT with phase of minimum BVI case being reduced from no AT case over a wade range of frequency, otherwise for AT with phase of maximum BVI case being increased, which is well agree to a tendency shown in Figs.8 and 9.

Blade surface pressure

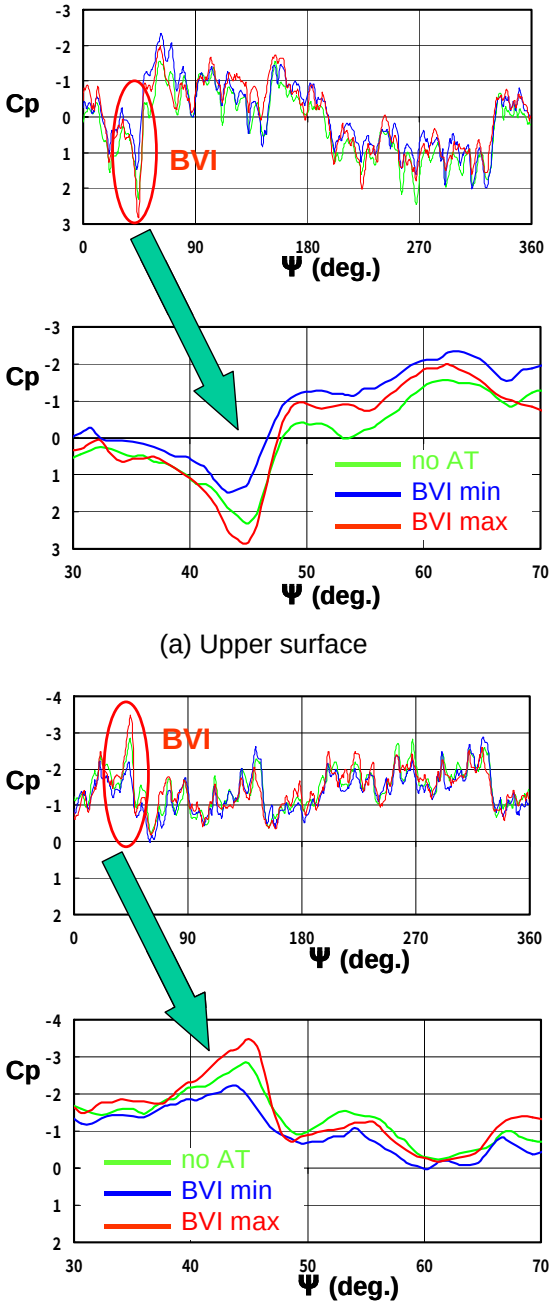

Fig.11 AT effect on blade surface pressure at 2.6%c, 85%R

V_W=18m/sec, rotor speed=600rpm, collective=4.3deg., cyclic=0deg., rotor shaft angle=2.0deg., AT frequency=2/rev, AT amplitude=3.8deg.

Fig.11 shows the blade surface pressure at 2.6%c, 85%R on the upper (Fig.11 (a)) and lower (Fig.11 (b)) surfaces with respect to the rotor azimuth of no AT and AT with phases for maximum and minimum BVI. In order to closely examine BVI phenomenon, the blade surface pressure over interested azimuth range around BVI region is magnified and shown in the lower halves of Fig.11 (a) and (b).

It is inferred based on these figures that the effective angle of attack of the blade segment is being decreased by the approach of the blade tip vortex and being increased by the departure, which makes the abrupt temporal change of the blade surface pressure. Fig.11 clearly shows this BVI phenomenon captured as this abrupt pressure change process in a short time of the period at around is ψ=45deg. for both the upper and lower sides of the blade. The difference in ψ's where BVI takes place between detected by Mic#1 (ψ=58deg, Fig.9) and by pressure transducers located on the 85%R of the blade (ψ=45deg, Fig.11) is caused by sound propagation time delay from the blade to Mic#1, which can be well explained based on speed of sound, rotor speed and a geometric relationship between Mic#1 and the blade.

Fig.11 also shows the effect of AT on the blade surface pressure as the difference in the magnitudes of Cp gap at around BVI region among no AT and AT with phases for maximum and minimum BVI. The tendency of Cp gap magnitudes, BVI max>no AT>BVI min, is obtained, which is similar to that of sound pressure as shown in Fig.9.

The magnitude of Cp gap at the BVI region has the difference between AT on and off. There also is this Cp gap difference among AT phases. Therefore, this Cp gap can be an index to express BVI relief effect due to AT phase variation.

In order to evaluate this BVI relief effect with respect to AT phase, the pressure fluctuation index Δ Cpmax which physically means the maximum value of the difference in the pressure coefficient between the successive ψ 's is introduced and defined as shown in Ref.8, which is repeated below for convenience.

$$\text{Pr}\,essure\,Fluctuation\,Index: \Delta C_{p\max} = \max(\Delta C_p(\psi_i))$$

$$\Delta C_p(\psi_i) = C_p(\psi_i) - C_p(\psi_{i-1})$$

$$\psi_i - \psi_{i-1} = 0.9\,\text{deg}.$$

$$C_p = \frac{P - P_s}{q}$$

where

P : measured blade surface pressure

Ps : static pressure

q :dynamic pressure at 85%R as V_W=0m/sec, rotor speed=600rpm

Fig.12 shows the blade surface pressure characteristics at 2.6%c, 85%R reduced in ΔCp over the interested ψ range on the upper (Fig.12 (a)) and lower (Fig.12 (b)) surfaces for no AT and AT with phases for maximum and minimum BVI.

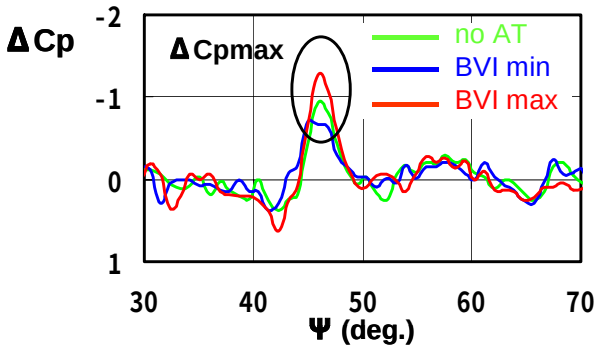

(a) Upper surface

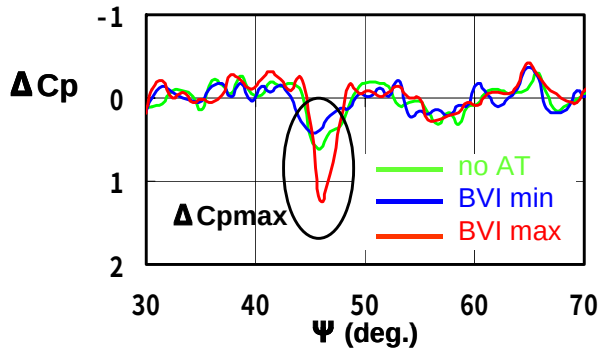

(b) Lower surface

Fig.12 Blade surface pressure fluctuation at 2.6%c, 85%R

V_W=18m/sec, rotor speed=600rpm, collective=4.3deg., cyclic=0deg., rotor shaft angle=2.0deg., AT frequency=2/rev, AT amplitude=3.8deg.

ΔCpmax of AT with phase of minimum BVI case is reduced from that of no AT case and ΔCpmax of AT with phase of maximum BVI case is larger than that of no AT case. This tendency can be seen on both the upper and lower surfaces of the blade.

Although ΔCpmax is obtained at ψ where the BVI takes place, there is some difference in ψ having ΔCpmax among these three cases in such a manner that BVI min the earliest, then no AT and BVI max the latest. Consequently, this also occurs on the sound pressure measurement as shown in Fig.9. The rotor azimuth angle at BVI depends on the position where the tip vortex and the blade collide with or have a minimum miss distance between each other. It is inferred that these positions for the three cases are varied by the wavy tip vortex trajectory made by AT activation and by the difference in its phase angles.

For more spatially macroscopic study of Δ Cp characteristics, the 85%R chordwise distribution of ΔCp at BVI for no AT and AT with phases for maximum and minimum BVI is shown in Fig.13. Because the BVI position varies case by case as mentioned above, the rotor azimuth angle between 45.9 to 46.8deg. is selected to present ΔCp in this figure for convenience.

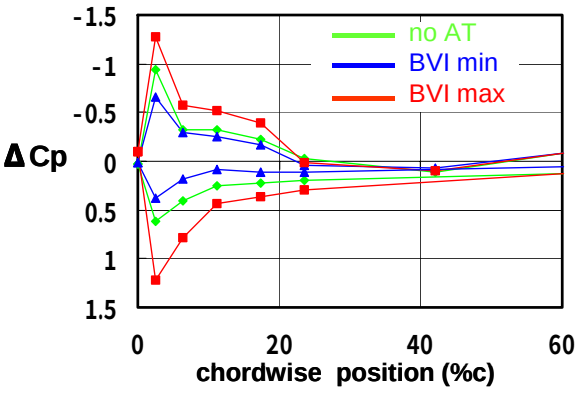

Fig.13 85%R Chordwise distribution of ΔCp at BVI

V_W=18m/sec, rotor speed=600rpm, collective=4.3deg., cyclic=0deg., rotor shaft angle=2.0deg., AT frequency=2/rev, AT amplitude=3.8deg.

The tendency of ΔCp, BVI max>no AT>BVI min, is obtained over the whole range of the blade chord, especially large values of ΔCp can be seen at the chordwise position close to the leading edge of the blade. This makes it sure that observing temporal variation of Cp at this portion is effective to detect BVI occurrence and to evaluate AT effect on BVI alleviation.

More systematic study for the effect of AT phase on ΔCp is shown in Fig.14 as the relationship between ΔCpmax and the whole range of AT phase. The minimum absolute value of ΔCpmax is obtained at AT phase=100deg., which means the maximum BVI relief effect is attained at this AT phase. The opposite happens at AT phase=282deg. where the most adverse influence of AT phase on BVI is observed.

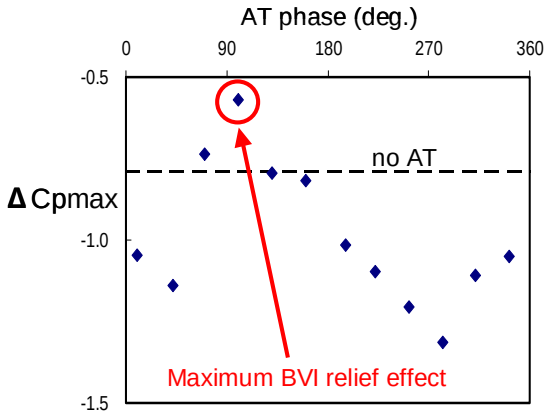

Fig.14 AT phase effect on ΔCpmax at 2.6%c, 85%R

V_W=18m/sec, rotor speed=600rpm, collective=4.3deg., cyclic=0deg., rotor shaft angle=2.0deg., AT frequency=2/rev, AT amplitude=3.8deg.

Correlation between sound pressure and blade surface pressure

As shown in Figs.9 (sound pressure), 11(Cp)and 12 (ΔCp), these three cases for no AT and AT with phases for maximum and minimum BVI share the common property to influence the degree of BVI with respect to AT phase.

Studying Figs.8 and 14 together, the correlation between the sound pressure level and ΔCpmax with respect to AT phase can be seen. AT phase range around 90deg. simultaneously has the largest rotor noise reduction indicated by the sound pressure level and the maximum BVI relief effect by ΔCpmax. On the other hand, the

opposite happens in AT phase range around 270deg. This characteristic of ∆Cpmax with respect to AT phase is useful as an input to the control law for Active Tab, because the BVI can be detected and evaluated by only on-board sensors.

Conclusions

Summarizing the experimental results, the followings are concluded by this study.

1. The strong correlation between blade surface pressure and sound pressure as to BVI with respect to Active Tab phase is obtained.

2. This implies that the blade surface pressure near the leading edge of the blade, which reacts sensitively to the degree of BVI intensity, can be a promising index to detect BVI and to evaluate AT effect on BVI reduction.

3. ∆Cpmax, temporal variation of blade surface pressure, near the leading edge of the blade can be utilized as an input to the control law for Active Tab.

Acknowledgements

The authors wish to express their thanks to Mr. Kosaka of Nihon University for his assistance to carrying out the wind tunnel testing and to data processing presented in this paper.

References

1. Hasegawa, Y., Katayama, N., Kobiki, N., Nakasato, E., Yamakawa, E., Okawa, H., “Experimental and Analytical Results of Whirl Tower Test of ATIC Full Scale Rotor System”, 57th Annual Forum of American Helicopter Society, Washington D.C., May 9-11, 2001.

2. Straub, F., Kennedy, D., “Design, Development, Fabrication and Testing of an Active Flap Rotor System”, 61st Annual Forum of American Helicopter Society, Grapevine, TX, June 1-3, 2005.

3. Enenkl, B., Klöppel, V., Preißler, D., “Full Scale Rotor with Piezoelectric Actuated Blade Flaps”, 28th European Rotorcraft Forum, Bristol, United Kingdom, September 17-19, 2002.

4. Fürst, D., Keßler, C., Auspitzer, T., Müller, M., Hausberg, A., Witte, H., “Closed Loop IBC-System and Flight Test Results on the CH-53G Helicopter”, 60th Annual Forum of American Helicopter Society, Baltimore, MD, June 7-10, 2004.

5. Kobiki, N., Kondo, N., Saito, S., Akasaka, T., Tanabe, Y., “Active Tab, a New Active Technique for Helicopter Noise Reduction”, 29th European Rotorcraft Forum, Friedrichshafen, Germany, September 16-18, 2003, Paper #50.

6. Aoyama, T., Yang, C., Saito, S., “Numerical Analysis of BVI Noise Reduction by Active Tab”, 60th American Helicopter Society Annual Forum, Baltimore, MD, June 7-10, 2004.

7. Kobiki, N., Kondo, N., Saito, S., Akasaka, T., Tanabe, Y., “An Experimental Study of On-blade Active Tab for Helicopter Noise Reduction”, 30th ERF, France, September, 2004.

8. Kobiki, N., Tsuchihashi, A., Murashige A., Yamakawa, E., “ Elementary Study for the Effect on HHC and Active Flap on Blade Vortex Interaction ”, 23rd European Rotorcraft Forum, Dresden , Germany, September 1997, Paper 29.